J Electr Eng Technol Vol. 7, No. 6: 1014-1022, 2012
http://dx.doi.org/10.5370/JEET.2012.7.6.1014

ISSN(Print) 1975-0102
ISSN(Online) 2093-7423

Finite Wordlength Recursive Sliding-DFT for Phase Measurement

Byoung-Il Kim*, Min-Kyu Cho* and Tae-Gyu Chang†

Abstract – This paper proposes a modified recursive sliding DFT to measure the phase of a single-tone. The modification is to provide a self error-cancelling mechanism so that it can significantly reduce the numerical error, which is generally introduced and accumulated when a recursive algorithm is implemented in finite wordlength arithmetic. The phase measurement error is analytically derived to suggest optimized distributions of quantization bits. The analytic derivation and the robustness of the algorithm are also verified by computer simulations. It shows that the maximum phase error of less than 5×10^{-2} radian is obtained even when the algorithm is coarsely implemented with 4-bit wordlength twiddle factors.

Keywords: Quantization effect, Roundoff analysis, Sliding DFT, Phase measurement.

1. Introduction

Sliding DFT is one of the effective methods to measure the single-tone phase in harmonically-distorted environment like electric power line systems[1-4]. This effectiveness is related to the harmonics decomposing characteristics of the DFT, where signals are directly decomposed into orthogonal harmonics of the fundamental component [4-6]. However, the computational complexity of DFT is often considered too high for the purpose of real time applications in a small scale embedded system. Recursive implementation of the sliding DFT can be considered as a means to reduce the computational complexity, if the recursive architecture can be free from the problem of accumulating finite-precision errors[6-8].

This paper proposes a modified recursive sliding DFT algorithm for measurement of single-tone phase. It is obtained by multiplying a phasor factor, which is rotating in the opposite direction, to the conventional recursive sliding DFT. This modification brings the use of quadruplet symmetric twiddle factors in its computation, consequently resulting in cancelling of the errors and its accumulation caused by the finite wordlength implementation. The error cancelling mechanism is described in section II.

The effect of finite wordlength implementation is analytically derived in section III to show its robustness against the finite-precision arithmetic in tracking the phase of a signal having frequency drift. The quantization effects are geometrically investigated to obtain the bounds of phase measurement error in a form of closed-function. The variance of the finite-precision error shows a quadratic nature in terms of the input and the twiddle factor quantization, which can be further exploited to derive optimized assignments of quantization wordlengths under given constraints of total number of representation bits. The optimized quantization architecture developed in this paper can serve as a useful design guide for the modified recursive sliding-DFT algorithm, especially for low complexity real-time phase measurement of a single-tone signal. The analytic derivations are also verified with the results of simulations performed for the phase tracking of power line signal.

† Corresponding author: Dept. of Electrical and Electronics Engineering, Chung-Ang University, Korea. (tgchang @cau.ac.kr)
* Dept. of Electrical and Electronics Engineering, Chung-Ang University, Korea. (savart@hanmail.net, minkyu413.cho @lge.com)
Received: July 13, 2012; Accepted: September 26, 2012

2. Modified Sliding-DFT Algorithm for Measurement of Single-Tone Phase

This section describes the proposed modified recursive algorithm to measure the phase of single-tone signals and to eliminate the error-accumulation phenomenon caused by the finite wordlength implementation.

Consider a single-tone signal of frequency $2\pi/M$ expressed as

$$x(n) = A_x \cos(\frac{2\pi}{M} n + \phi) \tag{1}$$

where A_x is the magnitude of the signal and ϕ is the phase of the signal as shown in Fig. 1.

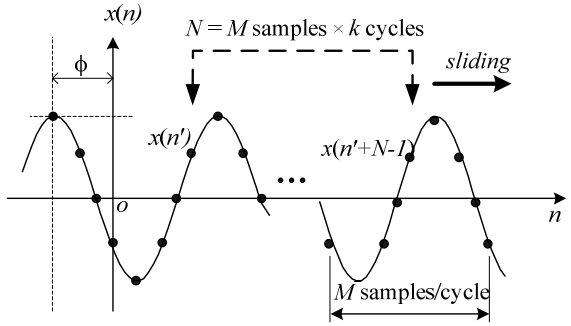

Fig. 1. Sliding window to measure the phase of a single-tone signal

The phasor of the signal $x(n)$ at the trailing edge of the sliding window, i.e., at $n'-N+1$ can be obtained from the k-th bin frequency component of DFT of the k cycle signal samples inside the sliding window in Fig.1, and which is defined as $X_k(n')$ in the following.

$$\begin{aligned} X_k(n') &\triangleq \sum_{m=0}^{N-1} x(m+n'-N+1)e^{\frac{-j2\pi km}{N}} \\ &= \sum_{m=0}^{N-1} A_x \cos(\frac{2\pi}{M}(m+n'-N+1)+\phi)e^{-j\frac{2\pi km}{kM}} \\ &= \sum_{m=0}^{N-1} \frac{A_x}{2}\left(e^{j\left[\frac{2\pi}{M}(m+n'-N+1)+\phi\right]} + e^{-j\left[\frac{2\pi}{M}(m+n')-N+1+\phi\right]} \right) e^{-j\frac{2\pi m}{M}} \\ &= \frac{A_x}{2}\sum_{m=0}^{N-1} e^{j\left[\frac{2\pi(n'-N+1)}{M}+\phi\right]} \\ &= \frac{NA_x}{2} e^{j\left(\frac{2\pi}{M}(n'-N+1)+\phi\right)} \end{aligned} \quad (2)$$

It is confirmed from (2) that $X_k(n')$ is same as the phasor of $x(n)$ at $n'-N+1$ except the DFT scaling factor $N/2$.

From now, for notational convenience, the variable n' is replaced with n to indicate the leading edge of the sliding window. Thus the phasor $X_k(n)$ indicates the signal phasor at the trailing edge of the sliding window, i.e., at $n-N+1$, and n indicates the leading edge of the window.

The recursive SDFT can be derived by relating $X_k(n)$ and $X_k(n-1)$ as shown in the following.

$$\begin{aligned} X_k(n) &\triangleq \sum_{m=0}^{N-1} x(m+n-N+1)e^{\frac{-j2\pi km}{N}} \\ &= \sum_{m=1}^{N} x(m-1+n-N+1)e^{\frac{-j2\pi k(m-1)}{N}} \\ &= e^{\frac{j2\pi k}{N}}\left[\sum_{m=0}^{N-1} x(m+n-1-N+1)e^{\frac{-j2\pi km}{N}} + x(n)-x(n-N)\right]. \end{aligned} \quad (3)$$

In the last line of (3), the first summation term in the bracket is equal to $X_k(n-1)$, therefore, the recursive sliding DFT equation is obtained as,

$$X_k(n) = W_N{}^k[X_k(n-1)+x(n)-x(n-N)], \quad (4)$$

where, W_N indicates the complex twiddle factor $e^{j(2\pi/N)}$.

The recursive SDFT given in (4) suffers from the severe error accumulation when the twiddle factors are represented by finite number of bits [6]. Repeated multiplication with the single quantized twiddle factors $\hat{W}_N^k$ will cause error accumulation. The error accumulation can be eliminated by modifying the phasor $X_k(n)$ to include W_N^{-kn} as defined in (5), which actually compensates the phasor rotation resulting from the window sliding.

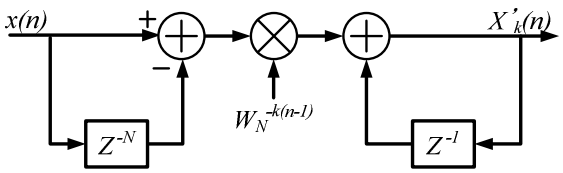

Fig. 2. The recursive implementation of the modified SDFT proposed for measuring the phase of single-tone signals.

$$X'_k(n) = X_k(n)W_N^{-kn} \quad (5)$$

By inserting (5) into (4), the recursive computation of the modified SDFT $X'_k(n)$ is obtained as (6) and its signal flow diagram is shown in Fig.2, respectively.

$$X'_k(n) = X'_k(n-1) + W_N^{-k(n-1)}[x(n)-x(n-N)] \quad (6)$$

As illustrated in Fig. 2, the arithmetic structure of the modified recursive SDFT is organized with the cascade of a finite impulse response (FIR) filter section and an infinite impulse response (IIR) filter section. In contrast to (4), where only a single fixed twiddle factor W_N^k is repeatedly used, the recursive computation of $X'_k(n)$ in (6) uses multiple numbers of twiddle factors which are quadruplet symmetric. The quadruplet symmetric characteristics of N twiddle factors provides the self error-canceling effect to eliminate the error accumulation, which will be analytically proved in Section III.

3. Analysis of Phase Error Caused by Finite Wordlength Implementation

This section analytically shows that the modified recursive SDFT is robust against the finite-precision arithmetic errors in tracking the phase of a tone signal having frequency drift. For the geometric evaluation of the phase error, the SDFT in (6) is first solved and obtained as the sum of two rotating phasors as shown in the following.

The modified recursive SDFT equation (6) can be represented equivalently in a non-recursive form as

$$X_k(n) = \sum_{m=0}^{n} W_N^{-k(m-1)}[x(m)-x(m-N)], \quad (7)$$

Where, and also in the following, the apostrophe in $X'_k(n)$ is dropped for notational simplicity.

Consider the input tone at frequency $f+\Delta f$ given as,

$$x(n) = A_x \cos(\frac{2\pi(f+\Delta f)}{f_s}n+\varphi), \quad (8)$$

where, the frequency Δf indicates the frequency deviation

of the input tone from its nominal frequency f, and f_s indicates the sampling frequency. Then the difference $x(n)-x(n-N)$ also becomes a sinusoidal signal at the same frequency $f+\Delta f$ as,

$$x(n)-x(n-N)=A_d\cos(\frac{2\pi(f+\Delta f)}{f_s}n+\varphi'), \qquad (9)$$

where, $A_d=A_x\sqrt{2(1-\cos[2\pi k(1+\Delta f/f)]}$ and φ' is the cumulative term.

By substituting (9) into (7), the phasor is derived to have the sum of two rotating phasors as

$$X_k(n)\approx A_p(\frac{1}{\gamma}e^{j(\frac{2\pi\Delta f}{f_s}n+\phi)}+\frac{1}{2+\gamma}e^{-j(\frac{2\pi(2f+\Delta f)}{f_s}n+\phi)}), \qquad (10)$$

where $A_p=A_dM/4\pi$, $\gamma=\Delta f/f$, $\phi=\varphi'-\pi/2$, and it is assumed that $\gamma\ll 1.0$. The detailed derivation of (9) and (10) is given in Appendix A and B, respectively.

Based on the phasor representation derived in (10), the finite wordlength effects can be obtained by geometrically evaluating their distributions in the complex plane.

The quantized input and the twiddle-factor can be represented as, $\hat{x}(m)=x(m)+q_x(m)$ and $\hat{W}_N^{-km}=W_N^{-km}+q_W(m)$, respectively. Where, $q_x(m)$ and $q_W(m)$ indicate the input quantization error and twiddle factor quantization error, respectively.

With the use of quantized input and twiddle factor, the DFT of the window data is approximated as

$$\hat{X}_k(n)=\sum_{m=0}^{N-1}\hat{x}(m+n-N+1)\hat{W}^{-km}. \qquad (11)$$

Neglecting the cross-product term between $q_x(m)$ and $q_W(m)$ in (11), the effects of input quantization and the twiddle-factor quantization can be separately investigated by defining $\hat{X}_k(n)$ as (12).

$$\hat{X}_k(n)=X_k(n)+E_x(n)+E_W(n) \qquad (12)$$

where $E_x(n)=\sum_{m=0}^{N-1}W_N^{-km}q_x(m+n-N+1)$, and $E_W(n)=\sum_{m=0}^{N-1}q_W(m)x(m+n-N+1)$.

2.1 Phase error caused by the input quantization

When the single-tone input is represented as b_x-bit binary word, the phasor, $\hat{X}_k$, can be represented as a composition of the true phasor X_k and the error phasor E_x as shown in (12) and its trajectory is shown in the complex plane in Fig. 3. The error phasor, E_x is spatially distributed around the true phasor. It is shown in Fig.3 that the phase error θ_x is caused by the perpendicular component of the phasor error E_x in reference to the direction of true phasor X_k.

Under the assumption that $|E_{xp}|/|X_k|\ll 1.0$, the variance of the phase error θ_x is obtained as the ratio between the expected values of $|E_{xp}|^2$ and $|X_k|^2$, i.e., $\sigma_{\theta x}^2=\varepsilon\{|E_{xp}|^2\}/\varepsilon\{|X_k|^2\}$, where, the notation $\varepsilon\{\cdot\}$ indicates the operation of the expectation.

Assuming the uniform distribution of the phasor error E_x around X_k, the perpendicular component $\varepsilon\{|E_{xp}|^2\}$ is obtained as half of $\varepsilon\{|E_x(n)|^2\}$ as follows.

$$\varepsilon\{|E_{xp}|^2\}=\frac{1}{2}\varepsilon\{|E_x(n)|^2\}=\frac{1}{2}\varepsilon\left\{\left|\sum_{m=0}^{N-1}W_N^{-km}q_x(m+n-N+1)\right|^2\right\}$$
$$=\frac{1}{2}\varepsilon\left\{\left[\sum_{m=0}^{N-1}W_N^{-km}q_x(m+n-N+1)\right]\left[\sum_{m=0}^{N-1}W_N^{km}q_x(m+n-N+1)\right]\right\}. \qquad (13)$$

Since $q_x(m)$ is uncorrelated random, the last line in (13) is further reduced as

$$\frac{1}{2}\varepsilon\left\{\left[\sum_{m=0}^{N-1}W_N^{-km}q_x(m+n-N+1)\right]\left[\sum_{m=0}^{N-1}W_N^{km}q_x(m+n-N+1)\right]\right\}$$
$$=\frac{1}{2}\varepsilon\left\{\sum_{m=0}^{N-1}q_x{}^2(m+n-N+1)\right\}=\frac{1}{2}\left\{\sum_{m=0}^{N-1}\varepsilon\{q_x{}^2(m+n-N+1)\}\right\}$$
$$=\frac{1}{2}\left\{\sum_{m=0}^{N-1}\sigma_{qx}{}^2\right\}=\frac{N}{2}\sigma_{qx}{}^2=\frac{N}{2}\frac{\Delta_x{}^2}{12},$$

where, $\sigma_{qx}{}^2$ is the power of the quantized noise of the input assuming its secondary order stationary.

Also, from (10), $\varepsilon\{|X_k|^2\}\approx(A_dM/4\pi\gamma)^2$. Therefore,

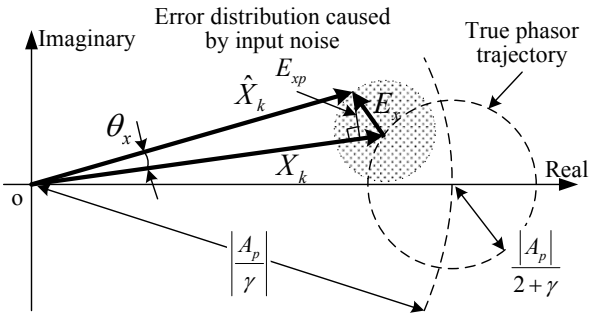

Fig. 3. Geometrical representation of the phase error caused by the finite wordlength representation of the input signal.

$$\sigma_{\theta x}^2 = \varepsilon\{|E_{xp}|^2\}/\varepsilon\{|X_k|^2\} = (2/3N)(k\pi\gamma\Delta_x/A_d)^2 \quad (14)$$

where, without loss of generality A_x is assumed to be 1.0, and then $\Delta_x = 2^{1-b_x}$.

If the bin frequency of DFT k is selected as one, i.e., N=M, and γ converges to zero, i.e., the frequency deviation is negligible, then γ/Ad in (14) can be treated as $1/2\pi$. Then (14) can be simplified as

$$\sigma_{\theta x}^2 \approx \Delta_x^2/6N. \quad (15)$$

2.2 Phase error caused by the twiddle factor approximation

While $\hat{W}_N^{kn}$ is a pure single-tone sequence, the approximated $\hat{W}_N^{kn}$ can be regarded as a periodic sequence containing harmonics associated with the quantization of the twiddle factors. Therefore, $\hat{W}_N^{kn}$ can be represented with the discrete Fourier series as

$$\hat{W}_N^{kn} = \frac{1}{N}\sum_{l=0}^{N-1} a_l e^{j\frac{2\pi lf}{f_s}n}. \quad (16)$$

Because of the symmetric placement of the twiddle factors in the complex plane, the third harmonic component is the first non-zero term beyond the fundamental component a_1 in (16) and is far greater than the other higher harmonics. Therefore the term W_N^{-kn} can be further approximated as the sum of the fundamental and the third harmonic components as

$$\hat{W}_N^{-kn} \approx (a_1/N)e^{-j\frac{2\pi f}{f_s}n} + (a_3/N)e^{-j\frac{6\pi f}{f_s}n}. \quad (17)$$

Then by replacing $\hat{W}_N^{-k(n-1)}$ and $x(n)-x(n-N)$ with (17) and (9), respectively, the phasor $\hat{X}(n)$ of (7) can be approximately obtained as

$$\hat{X}(n) \approx A_q\left\{\frac{1}{\gamma}e^{j(\frac{2\pi\gamma}{M}n+\phi)} + \frac{1}{2+\gamma}e^{-j(\frac{2\pi(2+\gamma)}{M}n+\phi)} + \frac{a_3}{a_1}\left(\frac{1}{2-\gamma}e^{-j(\frac{2\pi(2-\gamma)}{M}n-\phi)}\right)\right\}, \quad (18)$$

where, $A_q = A_p a_1/N$.

The detailed derivation of (18) is given in Appendix C. With this derivation, (18) can be regarded as the accumulation after the product of the single-tone $x(n)-x(n-N)$ of frequency $f+\Delta f$ with the fundamental and the third harmonic components of frequencies f and $3f$, respectively.

Among the product terms, all the higher frequency components are eliminated because the magnitude of higher harmonics is much smaller than that of the third harmonics. Therefore, only the first dominant harmonic error term $2f-\Delta f$ is included in (18). The first and the second terms in (18) are identical with the true phasor $X_k(n)$ of (10) except the inclusion of the scaling factor a_1/N to its magnitude. Without loss of generality, the scaling factor A_q can be treated as 1.0 since the common magnitude scaling does not affect the analysis of the phase error.

Then, with the twiddle factors being represented as b_W bit binary word, the phase error θ_W appears as the angle deviation from the true phasor X_k. The deviation is caused by the error phasor, E_W, i.e., by the last term of (12). E_W encircles around the true phasor trajectory, which is represented by the first two terms of (18) as shown in Fig. 4. The approximated magnitudes of the true phasor and the error phasor are proportional to $1/\gamma$, and $(a_3/a_1)/(2-\gamma)$, respectively.

The variance of the phase deviation can be obtained by integrating the perpendicular component, E_p, around the circle as

$$\sigma_{\theta W}^2 = \varepsilon\left\{|E_p|^2\right\}/\varepsilon\left\{|X_k|^2\right\} = \frac{1}{2\pi}\int_0^{2\pi}\left(\frac{a_3}{a_1}\Big|_{b_W}\frac{1}{2-\gamma}\sin\phi\right)^2 d\phi/\left(\frac{1}{\gamma}\right)^2 \approx \frac{4-\pi}{48}\left(\frac{\gamma\,\Delta_W}{2-\gamma}\right)^2, \quad (19)$$

where, the harmonic error ratio, a_3/a_1 is approximated to have the Rayleigh distribution because the quantization errors of real and imaginary values of the twiddle factors are jointly distributed in the complex plane[10], i.e.,

$$(a_3/a_1)^2\big|_{b_W} \approx \frac{4-\pi}{2}\sigma_{wq}{}^2, \quad \sigma_{wq}{}^2 = \frac{\Delta_W{}^2}{12}, \quad \Delta_W = 2^{1-b_W}.$$

If the frequency deviation, Δf is sufficiently small

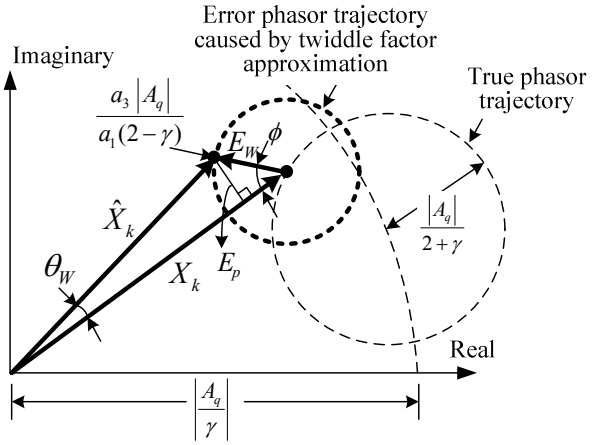

Fig. 4. Geometrical representation of the phase measurement error caused by the finite wordlength arithmetic of the twiddle factors.

relative to the nominal frequency f of the target signal x(n), the phase error in (19) is the quantization error power of twiddle factor, Δ^2_W scaled down with the near zero factor of $\gamma/(2-\gamma)$. This offers significant reduction of the phase measurement error caused by the finite wordlength twiddle factors.

For the finite wordlength implementation of both the input and the twiddle factors in the proposed phase detection algorithm, the variance of the phase error is obtained from (15) and (19) as

$$\sigma^2_{\theta e} = \sigma^2_{\theta x} + \sigma^2_{\theta w} = \frac{\Delta^2_x}{6N} + \frac{4-\pi}{48}\left(\frac{\gamma\,\Delta_W}{2-\gamma}\right)^2. \qquad (20)$$

2.3 Optimized selection of representation wordlength pairs

By further exploiting the quadratic expression of the error variance in (20), it is possible to provide optimized selections of the quantization wordlength pairs for the input and the twiddle factor of the recursive SDFT. For a given total number of bits, b_{tot}, to represent the input and the twiddle factor, the error variance shows a parabolic behavior for the different combination of representation wordlength pair as shown in Fig. 5.

From Fig. 5, it is found that, with the same b_{tot}, increment of the DFT block length results in a shift of the optimized quantization bit–pair, given as the minimum point of the parabolic curve, toward the lower-left direction. The shift indicates that smaller number of bits needs to be allocated for the input quantization and the saved number of bits can be additionally added to the quantization of the twiddle factor. This is the direct consequence coming from the fact that the input quantization noise decreases as the block length of the DFT increases. On the other hand, the optimized quantization bit-pair moves toward lower-right direction as the frequency drift ratio decreases as shown in Fig. 5. Optimized point's shift to the right hand direction indicates that the twiddle factor quantization needs to be more precise as the input tone signal contains more frequency drift.

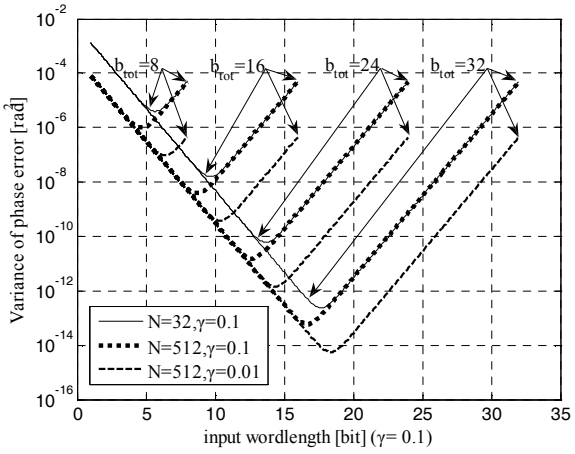

Fig. 5. Parabolic behaviors of the error variance for different combinations of the representation wordlength pairs. (SDFT block length N=32 and 512 at γ =0.1, and frequency drift ratio γ=0.1 and 0.01 at N=512.)

The optimized selection of b_x can be obtained by finding the minima of (20) by solving the following equation,

$$\frac{d\sigma^2_{\theta e}}{db_x} = \frac{d}{db_x}\left(4^{1-b_x} + \frac{4-\pi}{48}\left(\frac{\gamma}{2-\gamma}\right)^2 4^{b_x - b_{tot}+1}\right) = 0. \qquad (21)$$

From the solution of (21) for b_x,

$$b_{x\_opt} = \frac{1}{4}\log_2\left(\frac{4^{b_{tot}}}{6N} \Big/ \left\{\frac{4-\pi}{48}\left(\frac{\gamma}{2-\gamma}\right)^2\right\}\right)$$
$$= \frac{1}{2}b_{tot} - \frac{1}{4}\log_2 N - \frac{1}{2}\log_2\left(\frac{\gamma}{2-\gamma}\right) + \frac{1}{4}\log_2\left(\frac{8}{4-\pi}\right), \qquad (22)$$

where $b_{tot} = b_x + b_W$.

This result gives the design strategy to decide the optimized distribution of the quantization bits between the input and the twiddle factors, although the utilization of (22) is limited to the selection of closer integer values. Basic principle of the bit distribution is to allocate more bits to the side which dominates in causing the errors. As the frequency drift of the input increases, more phase error is caused by the multiplication with the approximated twiddle factors while the error caused by the quantization noise of the input remains the same. Therefore it is advantageous to allocate more bits for the twiddle factor quantization. It is found from (22) that, for the increase of frequency drift by the order of 10, 1.6 more bits need to be allocated for the twiddle factor quantization whereas 1.6 less bits are allocated for the input quantization. The signal to quantization noise ratio of the input reduces inverse proportionally as the block length increases. Therefore, it is also advantageous to allocate more bits to the twiddle

Table 1. Examples of the optimized selection of the representation wordlength pairs

(b_x : bit length for input, b_w : bit length for twiddle factor)

Total bits	*N*=32, γ=0.1			*N*=512, γ=0.1			*N*=32, γ=0.01		
	b_x	b_w	error variance [rad]	b_x	b_w	error variance [rad]	b_x	b_w	error variance [rad]
8	6	2	1.75×10^{-5}	5	3	4.37×10^{-6}	7	1	1.72×10^{-6}
12	8	4	1.09×10^{-6}	7	5	2.73×10^{-7}	9	3	1.07×10^{-7}
16	10	6	6.82×10^{-8}	9	7	1.71×10^{-8}	11	5	6.73×10^{-9}
20	12	8	4.26×10^{-9}	11	9	1.07×10^{-9}	13	7	4.20×10^{-10}
24	14	10	2.66×10^{-10}	13	11	6.66×10^{-11}	15	9	2.62×10^{-11}
28	16	12	1.66×10^{-11}	15	13	4.16×10^{-12}	17	11	1.64×10^{-12}
32	18	14	1.04×10^{-12}	17	15	2.60×10^{-13}	19	13	1.02×10^{-13}

factors. From (22), it is found that 0.25 more bits corresponds to the doubling of the DFT block length.

The summary shown in Table 1 is the optimized quantization bit distribution between the input and the twiddle factors for the varying number of total bit length and three different operation cases.

3. Simulations and Results

Simulations are performed to verify the analytic derivation of the phase measurement error obtained in section III.

In many practical applications, the frequency drift and/or the harmonic distortions are phenomena of special interest in tracking the phase of a tone signal. A good example is the monitoring of 50/60Hz power system where the correct tracking of the fundamental component of power line signal is important under the intrusion of harmonic distortion and the frequency drift caused by sudden or abnormal fault situations [9, 11]. Input tone signal is generated to include up to 7th odd harmonics with the same amplitude and frequency drift ranging from 0.001 to 0.1 times of the nominal frequency. The number of bits to represent the input and the twiddle factors are changed widely from 4 to 16 in the simulation.

The summary of the simulations and their comparison with the analytic derivation are shown in Fig. 6. It is confirmed that the analytically derived phase errors agree well with the simulation results. The robustness of the modified recursive SDFT is also very well illustrated in Fig. 6 such that the standard-deviation of the phase error is less than 10^{-3} radian even under the coarse 4-bit representation

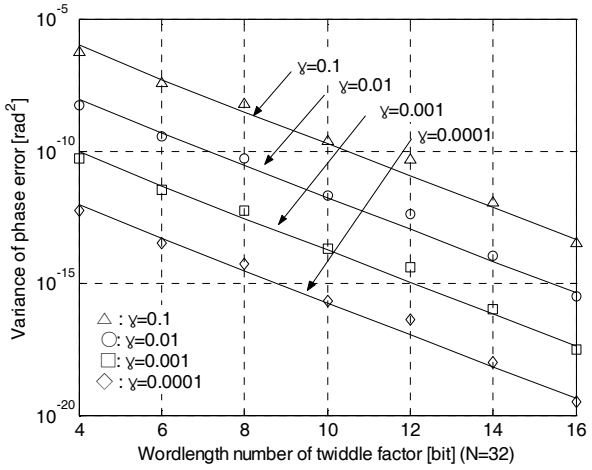

Fig. 6. Comparisons of the analytically derived phase errors with those obtained from simulations for different wordlength approximations of twiddle factors. The analytically derived results are illustrated with solid lines, and the simulation results are illustrated with the marks △, ○, □, and ◇.

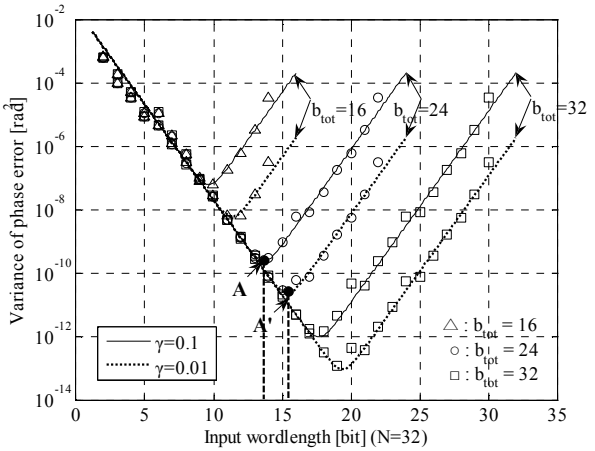

Fig. 7. Comparisons of the analytically derived phase errors with those obtained from simulations for different combinations of representation wordlength pairs, through the change of frequency drift ratio from γ=0.1 to γ=0.01.

of the DFT twiddle factor and the relatively significant amount of frequency drift (γ=0.1) in the input tone signal.

The parabolic behavior of the phase error variance, which is obtained by varying the distribution of the quantization bits between the input and the twiddle factor while the total number of quantization bits is kept constant, is well verified with the simulation results shown in Fig. 7. It is observed that the wordlength of twiddle factor is shorter by about four bits compared to those of input signal at the minimum error points, which indicates that the phase measurement is more robust with the twiddle factor approximation by about four bits in comparison with the input approximation. The minimum point's shift of 1.6-bit in the parabolic curves toward the right-hand direction (A to A') indicates the increased relative effect of the input quantization error as the frequency drift ratio decreases by the factor of ten, i.e., from 0.1 to 0.01.

4. Conclusion

This paper proposed a modified recursive sliding-DFT and showed its application to measuring the phase of a single-tone signal. The robustness of the proposed algorithm against the finite wordlength implementation was analytically derived and was verified with computer simulations as well. The analysis also showed the parabolic behavior of the performance error curve and its dependency on the effects of the frequency drift of the input, consequently suggesting for the optimized quantization architecture of the algorithm. The robustness of the modified recursive SDFT has been also well illustrated such that the standard-deviation of the phase error is less than 10^{-3} radian even under the coarse 4-bit representation of the DFT twiddle factor and the relatively

significant amount of frequency drift. It is concluded from this study that the modified recursive sliding-DFT can be regarded as a useful method to measure the phase of a single-tone signal, especially when the processing speed and implementation simplicity are critical considerations in the application.

Acknowledgements

This work was supported by the Excellent Research Assistant Support Grant of Chung-Ang University.

References

[1] A. P. Liavas and P. A. Regalia, "On the numerical stability and accuracy of the conventional recursive least squares algorithm," *IEEE Trans. Signal Processing*, Vol. 47, pp. 88-96, Jan. 1999.

[2] J.R. Bunch and R.C. LeBorne, "Error accumulation effects for the a posteriori RLSL prediction filter," *IEEE Trans. Signal Processing*, Vol. 43, pp. 150-159, Jan. 1995.

[3] E. Jacobsen and R. Lyons, "The sliding DFT," *IEEE Signal Processing Magazine*, Vol. 20, pp. 74-80, Mar 2003.

[4] E. Jacobsen and R. Lyons, "An update to the sliding DFT," *IEEE Signal Processing Magazine*, Vol. 21, pp. 110-111, Jan. 2004.

[5] K. P. Sozanski, "Sliding DFT control algorithm for three-phase active power filter," in *Conf. 21th Annual IEEE Applied Power Electronics Conference and Exposition*, pp. 1223-1229 March 2006.

[6] F. Beaufays and B. Widrow, "On the advantages of the LMS spectrum analyzer over nonadaptive implementations of the sliding-DFT," *IEEE Trans. Circuits and Systems I: Fundamental Theory and Applications*, Vol. 42, pp. 218-220, April 1995.

[7] J. H. Kim and T. G. Chang, "Analytic derivation of finite wordlength effect of the twiddle factors in recursive implementation of the sliding-DFT," *IEEE Trans. Signal Processing*, Vol. 48, pp. 1485-1488, May 2000.

[8] J. Z. Yang and C. W. Liu, "A precise calculation of power system frequency and phasor," *IEEE Trans. Power Delivery*, Vol. 15, pp. 494-499, April 2000.

[9] B.S. Ahn, B.I. Kim and T.G. Chang, "A sliding-DFT based power-line phase measurement algorithm and its FPGA implementation," in *Conf. 8th IEE Int. Conf. Developments in Power System Protection*, Vol. 1, pp 44-47, April 2004.

[10] G. Panda, R. Pal and B. Chatterjee, "On the effect of correlation between truncation errors in fixed-point error analysis of Winograd short-length DFT algorithms," *IEEE Trans. Acoustics, Speech, and Signal Processing*, Vol. 30, pp.100-104, Feb. 1982.

[11] T. Lin, and A. Jr. Domijan, "Recursive Algorithm for Real-Time Measurement of Electrical Variables in Power Systems," *IEEE Trans. Power Delivery*, Vol. 21, pp. 15-22, Jan. 2006.

Appendix A

From (8),

$$\begin{aligned} x(n)-x(n-N) &= A_x\cos(\tfrac{2\pi(f+\Delta f)}{f_s}n+\varphi)-A_x\cos(\tfrac{2\pi(f+\Delta f)}{f_s}(n-N)+\varphi) \\ &= A_x[\cos(\tfrac{2\pi(f+\Delta f)}{f_s}n+\varphi)-\cos(\tfrac{2\pi(f+\Delta f)}{f_s}n+\varphi)\cos(\tfrac{2\pi(f+\Delta f)}{f_s}N) \\ &\quad -\sin(\tfrac{2\pi(f+\Delta f)}{f_s}n+\varphi)\sin(\tfrac{2\pi(f+\Delta f)}{f_s}N)] \\ &= A_x\sqrt{(-\sin(\tfrac{2\pi(f+\Delta f)}{f_s}N))^2+(1-\cos(\tfrac{2\pi(f+\Delta f)}{f_s}N))^2} \\ &\quad \cdot\cos(\tfrac{2\pi(f+\Delta f)}{f_s}n+\varphi') \\ &= A_x\sqrt{2-2\cos(\tfrac{2\pi(f+\Delta f)}{f_s}N)}\cdot\cos(\tfrac{2\pi(f+\Delta f)}{f_s}n+\varphi'). \end{aligned} \quad (23)$$

In (23), the cumulative phase term φ' is replaced by ϕ for notational convenience, and N is replaced using $N=(f_s/f)k$, then (9) is obtained.

Appendix B

In (9), the cumulative phase φ' is replaced by φ for notational convenience and inserting (9) into (7),

$$\begin{aligned} X_k(n) &= \sum_{m=0}^{n} W_N^{-k(m-1)}[x(m)-x(m-N)] \\ &= \sum_{m=0}^{n} W_N^{-k(m-1)} A_d\cos(\tfrac{2\pi(f+\Delta f)}{f_s}m+\varphi) \\ &= \frac{A_d}{2}\sum_{m=0}^{n} e^{-j\frac{2\pi}{N}k(m-1)}[e^{j(\frac{2\pi(f+\Delta f)}{f_s}m+\varphi)}+e^{-j(\frac{2\pi(f+\Delta f)}{f_s}m+\varphi)}] \\ &= \frac{A_d}{2}\sum_{m=0}^{n}[e^{j(\frac{2\pi\Delta f}{f_s}m+\frac{2\pi f}{f_s}+\varphi)}+e^{-j(\frac{2\pi}{f_s}(2f+\Delta f)m-\frac{2\pi f}{f_s}+\varphi)}]. \end{aligned} \quad (24)$$

The first term in the last line of (24) is,

$$\begin{aligned} \frac{A_d}{2}\sum_{m=0}^{n} e^{j(\frac{2\pi\Delta f}{f_s}m+\frac{2\pi f}{f_s}+\varphi)} &= \frac{A_d}{2}e^{j\frac{2\pi f}{f_s}}e^{j\varphi}\sum_{m=0}^{n} e^{j\frac{2\pi\Delta f}{f_s}m} \\ &= \frac{A_d}{2}e^{j\frac{2\pi f}{f_s}}e^{j\varphi}\frac{1-(e^{j(2\pi\Delta f/f_s)})^{n+1}}{1-e^{j(2\pi\Delta f/f_s)}}. \end{aligned}$$

Since $|\Delta f/f_s|\ll 1.0$, $1-e^{j(2\pi\Delta f/f_s)}\approx -j(2\pi\Delta f/f_s)$. Then,

$$\frac{A_d}{2}e^{j\frac{2\pi f}{f_s}}e^{j\varphi}\frac{1-}{1-e^{j(2\pi\Delta f/f_s)}}\approx\frac{A_d}{2}e^{j\frac{2\pi f}{f_s}}e^{j\varphi}\frac{1-(e^{j(2\pi\Delta f/f_s)})^{n+1}}{-j2\pi\Delta f/f_s}$$
$$=A_p\frac{1}{\gamma}e^{j(\frac{2\pi\gamma}{M}n+\varphi-\frac{\pi}{2})}+\alpha,$$

where, $A_p=A_dM/4\pi$, $\gamma=\Delta f/f$, $f_s=fM$, and α represents the constant offset term of the rotating phasor.

The second term in the last line of (24) is obtained in the same way as,

$$\frac{A_d}{2}\sum_{m=0}^{n}e^{-j\left(\frac{2\pi}{f_s}(2f+\Delta f)m-\frac{2\pi f}{f_s}+\varphi\right)}=A_p\frac{1}{2+\gamma}e^{-j\left(\frac{2\pi}{M}(2+\gamma)n+\varphi-\frac{\pi}{2}\right)}+\beta,$$

where $A_p=A_dM/4\pi$ and β represents the constant offset term of the rotating phasor.

The constant offset terms α and β can be dropped since they commonly appear in both true and approximated phasor $X_k(n)$ and $\hat{X}_k(n)$, respectively, and under the condition $|\gamma|\ll 1.0$, the average phase estimation error is approximately same when measured only from the relationship among the rotating phasor terms. By summing the two terms, dropping the constant terms α and β, and replacing the cumulative phase $\varphi-\pi/2$ with ϕ for notational convenience, then (10) is obtained.

Appendix C

Insert (17) and (9) into (7),

$$\begin{aligned}X_k(n)&=\sum_{m=0}^{n}W_N^{-k(m-1)}[x(m)-x(m-N)]\\&=\sum_{m=0}^{n}\left[\frac{a_1}{N}e^{-j\frac{2\pi f}{f_s}(m-1)}+\frac{a_3}{N}e^{-j\frac{6\pi f}{f_s}(m-1)}\right]\\&\quad\cdot A_d\cos\left(\frac{2\pi(f+\Delta f)}{f_s}m+\varphi'\right)\\&=\sum_{m=0}^{n}\left[\frac{a_1}{N}e^{-j\frac{2\pi f}{f_s}(m-1)}+\frac{a_3}{N}e^{-j\frac{6\pi f}{f_s}(m-1)}\right]\\&\quad\cdot\frac{A_d}{2}\left[e^{j\left(\frac{2\pi(f+\Delta f)}{f_s}m+\varphi'\right)}+e^{-j\left(\frac{2\pi(f+\Delta f)}{f_s}m+\varphi'\right)}\right]\\&=\frac{A_d}{2}\sum_{m=0}^{n}\left[\begin{array}{l}\frac{a_1}{N}e^{j\left(\frac{2\pi\Delta f}{f_s}m+\frac{2\pi f}{f_s}+\varphi'\right)}+\frac{a_1}{N}e^{-j\left(\frac{2\pi}{f_s}(2f+\Delta f)m-\frac{2\pi f}{f_s}+\varphi'\right)}\\+\frac{a_3}{N}e^{-j\left(\frac{2\pi}{f_s}(2f-\Delta f)m-\frac{6\pi f}{f_s}-\varphi'\right)}+\frac{a_3}{N}e^{-j\left(\frac{2\pi}{f_s}(4f+\Delta f)m-\frac{6\pi f}{f_s}+\varphi'\right)}\end{array}\right]\end{aligned}\quad(25)$$

For the first term in the last line of (25),

$$\frac{A_d}{2}\sum_{m=0}^{n}\frac{a_1}{N}e^{j\left(\frac{2\pi\Delta f}{f_s}m-\frac{2\pi f}{f_s}+\varphi'\right)}=\frac{A_d}{2}\frac{a_1}{N}e^{j\frac{2\pi f}{f_s}}e^{j\varphi'}\sum_{m=0}^{n}e^{j\frac{2\pi\Delta f}{f_s}m}$$
$$=\frac{A_d}{2}\frac{a_1}{N}e^{j\frac{2\pi f}{f_s}}e^{j\varphi'}\frac{1-(e^{j(2\pi\Delta f/f_s)})^{n+1}}{1-e^{j(2\pi\Delta f/f_s)}}$$

Dropping the constant offset term and applying $1-e^{j(2\pi\Delta f/f_s)}\approx-j(2\pi\Delta f/f_s)$, then,

$$\begin{aligned}\frac{A_d}{2}\sum_{m=0}^{n}\frac{a_1}{N}e^{j\left(\frac{2\pi\Delta f}{f_s}m-\frac{2\pi f}{f_s}+\varphi'\right)}&=-\frac{A_d}{2}\frac{a_1}{N}e^{j\varphi'}\frac{e^{j\frac{2\pi\Delta f}{f_s}n}}{-j\frac{2\pi\Delta f}{f_s}}\\&=\frac{A_da_1}{4\pi N}\frac{f_s}{\Delta f}e^{j\left(\frac{2\pi\Delta f}{f_s}n+\varphi'-\frac{\pi}{2}\right)}\\&=A_q\frac{1}{\gamma}e^{j\left(\frac{2\pi\Delta f}{f_s}n+\phi\right)},\end{aligned}$$

where $f_s=fM$, $\gamma=\Delta f/f$, $\phi=\varphi'-\pi/2$, and $A_q=A_da_1M/4\pi N$.

The rest terms in (25) can be derived in the same way as

$$\frac{A_d}{2}\sum_{m=0}^{n}\frac{a_1}{N}e^{-j\left(\frac{2\pi}{f_s}(2f+\Delta f)m-\frac{2\pi f}{f_s}+\varphi'\right)}$$
$$=\frac{A_d}{2}\frac{a_1}{N}e^{j\frac{2\pi f}{f_s}}e^{-j\varphi'}\sum_{m=0}^{n}e^{-j\frac{2\pi}{f_s}(2f+\Delta f)m}\approx A_q\frac{1}{2+\gamma}e^{-j\left(\frac{2\pi}{M}(2+\gamma)n+\phi\right)},$$

$$\frac{A_d}{2}\sum_{m=0}^{n}\frac{a_3}{N}e^{-j\left(\frac{2\pi}{f_s}(2f-\Delta f)m-\frac{6\pi f}{f_s}-\varphi'\right)}$$
$$=\frac{A_d}{2}\frac{a_3}{N}e^{j\frac{6\pi f}{f_s}}e^{j\varphi'}\sum_{m=0}^{n}e^{-j\frac{2\pi}{f_s}(2f-\Delta f)m}$$
$$\approx A_q\frac{a_3}{a_1}\frac{1}{2-\gamma}e^{-j\left(\frac{2\pi}{M}(2-\gamma)n-\phi\right)},\text{ and}$$

$$\frac{A_d}{2}\sum_{m=0}^{n}\frac{a_3}{N}e^{-j\left(\frac{2\pi}{f_s}(4f+\Delta f)m-\frac{6\pi f}{f_s}+\varphi'\right)}$$
$$=\frac{A_d}{2}\frac{a_3}{N}e^{j\frac{6\pi f}{f_s}}e^{-j\varphi'}\sum_{m=0}^{n}e^{-j\frac{2\pi}{f_s}(4f+\Delta f)m}$$
$$\approx A_q\frac{a_3}{a_1}\frac{1}{4+\gamma}e^{-j(\frac{2\pi}{M}(4+\gamma)n-\phi)}.$$

By summing the three dominant phasor terms, (18) is obtained.

Byoung-Il Kim He received the B.S., M.S. and Ph.D. degrees from the Chung-Ang University, Seoul, Korea, in 2001, 2003, and 2007, respectively, all in electrical engineering. He is currently a senior engineer at the AP Development Team, System LSI Division, Samsung Electronics, Korea. His research interests are in the areas of multimedia signal processing, sytem LSI, and ASIC design.

Min-Kyu Cho He received the B.S. and M.S. degrees from the Chung-Ang University, Seoul, Korea, in 2010, and 2012, respectively, all in electrical engineering. He is currently a research engineer at HA Tech. Control Gr. HA Control R&D Lab., LG Electronics, Korea. His research interests are in the areas of multimedia signal processing and digital communications.

Tae-Gyu Chang He received the B.S. degree from the Seoul National University, Seoul, Korea, in 1979, and M.S. degree from Korea Advanced Institute of Science and Technology, Seoul, in 1981, and Ph.D. degree from University of Florida, Gainesville, in 1987, all in electrical engineering. From 1981 to 1984, he was with the Hyundai Engineering/ Electronics Inc., Seoul, as a Systems Design Engineer. From 1987 to 1990, he was a Faculty Member of Tennessee State University, Nashville, as a Research Assistant Professor at the Center of Excellence in Information Systems Engineering and Management. In March 1990, he joined the faculty of the Chung-Ang University, Seoul, Korea where he is currently a Professor at the Department of Electrical and Electronics Engineering. His research interests include digital signal processing and communications.